MATHEMATICAL BIOSCIENCES
AND ENGINEERING
Volume **13**, Number **2**, April **2016**

doi:10.3934/mbe.2015005

pp. **333–341**

DIRECTIONAL ENTROPY BASED MODEL FOR DIFFUSIVITY-DRIVEN TUMOR GROWTH

Marcelo E. de Oliveira*

Robotic Systems Laboratory
Swiss Federal Institute of Technology (EPFL)
Lausanne, CH-1015, Switzerland

Luiz M. G. Neto

Department of Mechanical Engineering
Engineering College of Sorocaba (FACENS)
São Paulo, 18087-125, Brazil

(Communicated by Eugene Kashdan)

Abstract. In this work, we present and investigate a multiscale model to simulate 3D growth of glioblastomas (GBMs) that incorporates features of the tumor microenvironment and derives macroscopic growth laws from microscopic tissue structure information. We propose a normalized version of the Shannon entropy as an alternative measure of the directional anisotropy for an estimation of the diffusivity tensor in cases where the latter is unknown. In our formulation, the tumor aggressiveness and morphological behavior is tissue-type dependent, i.e. alterations in white and gray matter regions (which can e.g. be induced by normal aging in healthy individuals or neurodegenerative diseases) affect both tumor growth rates and their morphology. The feasibility of this new conceptual approach is supported by previous observations that the fractal dimension, which correlates with the Shannon entropy we calculate, is a quantitative parameter that characterizes the variability of brain tissue, thus, justifying the further evaluation of this new conceptual approach.

1. **Introduction.** Glioblastoma multiforme (GBM) is by far the most common and aggressive type of gliomas in humans, occurring most often in the subcortical white matter of the cerebral hemispheres. These tumors have drawn significant attention since most patients with GBMs die in less than a year and, despite extensive research, little advance in the treatment of GBMs has occurred in the last decades [19].

Understanding GBM dynamics and morphology based on computational modeling is of great interest to the scientific community because it offers the potential to both provide new fundamental insights into the phenomenon of cancer and to allow more realistic and accurate prediction of tumor evolution. A number of GBM growth models exist in the literature [3, 5, 10, 11, 17, 23, 12, 1, 20, 13, 22, 18]. However, for anisotropic models, diffusion tensor images (DTI) are required, which are not always easily accessible, especially in the case of model validation procedures

2010 *Mathematics Subject Classification.* Primary: 94A17, 62P10, 68U10; Secondary: 65M06, 37M10.

Key words and phrases. Glioblastomas, diffusivity tensor, Shannon entropy, fractal dimension.

* Corresponding author: Marcelo E. de Oliveira.

using legacy patient data. We therefore propose a model to estimate diffusivity properties based on information gained from concepts of information theory using magnetic resonance images (MRI) only.

The concept of fractal dimension (D_F) was introduced in 1982 by Mandelbrot [16] as a quantitative parameter that characterizes the morphometric variability of a complex object with widespread applications in the neuroscience field [8], serving e.g. as inter- and intra-feature descriptor of different cerebral tissue microstructures. In nonlinear dynamics, many specific fractal dimensions have been proposed. The most important theoretical fractal dimensions are the Hausdorff dimension, information dimension, box-counting dimension, and correlation dimension [21, 2]. Previous works have shown that the D_F is a sensitive metric to detect changes in white and gray matter induced by neurodegenerative diseases [6, 7, 14]. In 2004, Takahashi et al. [24] verified the morphological complexity variability of white matter in normal aging based on MRI datasets. Therefore, the variability of the morphological complexity of a cerebral structure is directly related to its D_F, thus this metric can be used as a surrogate marker for detecting brain tissue abnormalities, for distinguishing different cerebral structures and as well as an indicator of biological aging.

Another important quantity in information theory is the entropy, which quantifies the amount of information contained in a distribution. It has been shown in the literature that entropy and fractal dimension are related quantities. Microstructures containing well defined features exhibit lower fractal dimensions and consequently lower entropies. White matter is made up of oriented myelinated nerve fibers, thus, presenting lower morphometric complexity (i.e., lower D_F) [6, 7] and consequently lower entropy when compared to gray matter which is made up mostly of nerve cell bodies.

Part of our work is motivated by experimental observations made by Giese et al. (1996) [9] on the GBM invasion speed which plays an important role in the understanding of its dynamics. Results of this study indicated that the GBM growth rate depends of the invaded tissue microstructures and it was verified that tumor cells spread faster in white matter than in gray matter.

In the present work, we will first present the relationships between the generalized entropy and the information dimension. Thereafter, we will introduce the use of normalized directional Shannon entropies as an alternative measure of cerebral tissue diffusional anisotropy which may lead to additional important information about the tissue microstructure surrounding the GBM and patient-specific tumor behavior.

In summary, we calculate the generalized entropy of specific domains in the brain, which is correlated to the information dimension, which in turn has been shown to depend on gray matter/white matter content. These two main brain material constituents exhibit different tumor cell spread characteristics. Therefore, the generalized entropy in different direction segments offers the potential to characterize diffusivity properties for spreading tumor cells.

2. **Methods.**

2.1. **Generalized entropy and information dimension.**

A common way to calculate a fractal dimension is based on the Shannon entropy S_1 which is a particular case of the generalized Rényi entropy. Given a vector $X = \{x_1, x_2, \ldots, x_n\}$ with

probabilities $p_1, p_2, \ldots, p_n$, the generalized entropy of order α, where $\alpha > 0$ and $\alpha \neq 1$ is defined as [21]:

$$S_\alpha(X) = \frac{1}{(1-\alpha)} \log_2 \left(\sum_{i=1}^{n} p_i^\alpha \right), \tag{1}$$

In the limit for α going to 1 the generalized Rényi entropy converges to Shannon's entropy (by l'Hôpital's rule), and Eq. 1 becomes

$$S_1 = -\sum_{x=1}^{n} p_i \log_2(p_i), \tag{2}$$

The information dimension D_1 quantifies how the average information needed to identify an occupied box scales with size ε as the scale of boxes gets smaller. Its relationship to the Shannon entropy reads as follows [21]:

$$D_1 = -\lim_{\varepsilon \to 0} \frac{S_1}{\log_2(\varepsilon)} \tag{3}$$

2.2. **Directional-dependent entropy calculation.** In this subsection we describe the proposed approach for the calculation of the anisotropic information comprising the source volume Ω, i.e., microstructures existing in the region of interest (ROI) surrounding the GBM (Fig. 1a). The proposed conceptual approach has been evaluated on a T2-weighted magnetic resonance (MR) data set acquired from a healthy male subject, 46 years old. For illustrative purposes, the origin of the tumor was assumed to be localized in the right anterior temporal lobe and centered in the cubic grid containing all $N = 27$ subdomains Γ (Fig. 1b). Each subdomain is divided into six volumetric sectors in which is uniquely determined by the intersection of a sphere of radius r with a cone, where the apex of the cone coincides with the center of the sphere (Fig. 1d). The volumetric sectors of each subdomain are oriented along the directions X^+, X^-, Y^+, Y^-, Z^+ and Z^- in the image space (Figs. 1c-1e). The information content of each volumetric sector was extracted by binning the voxel intensities (grayscale levels) into 256 quantized levels, and their probabilities p_i were assessed by computing the total number of voxels intensities into their respective bins divided by the total number of voxels confined into all N subdomains Γ. In real world data, there always exists a small enough r greater than the voxel size which will yield approximately the same entropy for basic elements facing opposite directions, i.e., $S_1^{+x} \approx S_1^{-x}$, $S_1^{+y} \approx S_1^{-y}$, and $S_1^{+z} \approx S_1^{-z}$ since the same microstructure will be present in an infinitesimal symmetric sector around each grid point. This procedure allows the calculation of the directional entropies and the characterization of different microstructures surrounding the ROI. Finally, the mean directional entropies for each subdomain Γ_n were computed as follow: $S_1^\zeta = (S_1^{+\zeta} + S_1^{-\zeta})/2$, for $\zeta = 1$, 2, and 3.

2.3. **Diffusivity model.** In the late 1980s, Murray et al. [17] presented a model to describe the diffusion of cancer cells through brain tissue. This model consists of a partial differential equation which describes concentration fluctuations of cancer cells through cerebral tissues and is usually written as

$$\frac{\partial c(x,t)}{\partial t} = \nabla \cdot (D(x) \nabla c(x,t)) + \rho(x,t) c(x,t), \tag{4}$$

where $c(x,t)$ is the concentration of the diffusing cancer cells at location (x, y, z) and time t, $D(x, y, z)$ is the diffusion tensor, and $\rho(x,t)$ represents the rate of growth

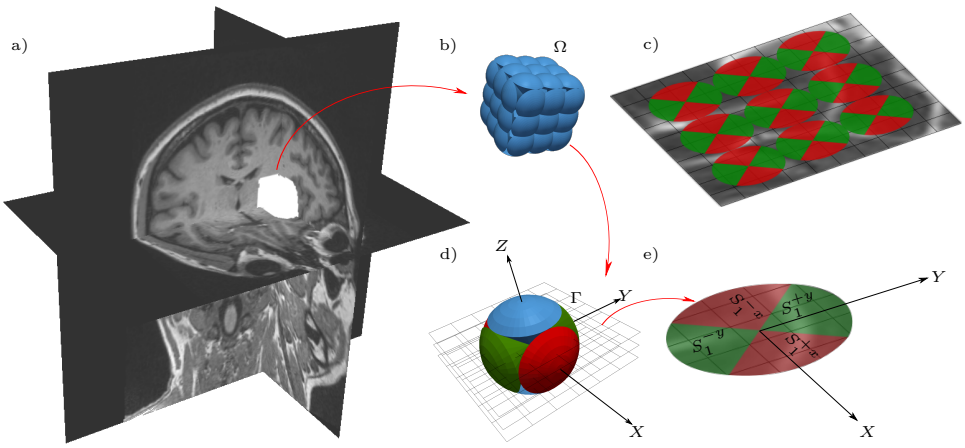

FIGURE 1. Characterization of the anisotropy based on the directional Shannon entropies for estimation of the diffusivity tensor. a) For visualization purposes, the levels for the voxels comprising the ROI were modified. b) Cubic grid containing $N = 27$ subdomains. c) Projection of the 3D-data confined in the ROI Ω onto an image plane for visualization of changes of tissue microstructure. d-e) Subdamin composed of six volumetric sectors. The information confined into these structures are used to estimate the directional entropies in the X, Y, and Z directions, which are depicted in red, green and blue colors, respectively.

of cells (cell proliferation and cell loss) in its specific brain location. An important characteristic to be observed is that in anisotropic media the diffusion tensor is a function of its spatial location, characterizing the microscopic tissue structure, as shown in Eq. 5).

$$\frac{\partial c(x,t)}{\partial t} = \sum_{i,j=1}^{3} \left(\frac{\partial D_{ij}(x)}{\partial x_i} \frac{\partial c(x,t)}{\partial x_j} + D_{ij}(x) \frac{\partial^2 c(x,t)}{\partial x_i \partial x_j} \right) + \rho(x,t) c(x,t) \tag{5}$$

The tumor origin (most active region) is assumed to be centered in the defined ROI Ω, and it has been used as a source-volume for the diffusion of cancer cells with a maximum cancer cell holding capacity estimated to be $C_{max} = 10^4$ cells mm^{-3} [25, 17, 4]. C_{max} was used for normalizing the calculated concentrations, consequently, the concentrations range from 0 to 1. A cell production rate equivalent to 1% of C_{max} has been assumed in our simulations. Zero-flux boundary conditions were assumed for the elements located at the boundary surface $\partial\Omega$ delimited by the source volume Ω.

$$\mathbf{n} \cdot D(x) \nabla c(x,t) = 0, \ \forall x \in \partial\Omega \tag{6}$$

where $\mathbf{n}$ is an outer unit vector normal to the boundary $\partial\Omega$ of Ω.

2.4. **Diffusivity tensor estimation from normalized directional entropies.** As previously discussed, microstructures containing well defined features exhibit relatively lower entropies and higher diffusivity. Thus, a linear relationship between the directional entropies and diffusivity was assumed, mapping the infimum $\inf\{S_1^{\zeta}\}$

to the highest and the supremum $\sup\{S_1^\zeta\}$ to the lowest diffusivity, respectively. Previous studies have shown that cancer cells diffuse faster in white matter than in gray matter [9], suggesting that the diffusivity in gray matter is a fraction of the experimentally observed maximum diffusivity in white matter ($D_{WM} = 10^{-3} mm^2 s^{-1}$). Therefore, the diffusivity in gray matter is defined as $D_{GM} = \beta \times D_{WM}$ and in our simulations we assumed $\beta = 1/100$ which is in accordance with previous studies [17, 25]. The directional entropies at non-grid positions in the domain Ω were evaluated by using the bicubic interpolation method, and the volume space comprising the ROI was discretized and the PDEs (Eqs. 5 and 6) were solved by using the forward-time central space method (FTCS) [15]. The proposed method for diffusivity-driven tumor growth modelling is summarized below:

Diffusivity-driven tumor growth modelling

1: Definition of the source volume Ω surrounding the GBM by using a grid containing N subdomains Γ (Figs. 1a-1b)
2: Evaluation of the directional entropies for all N subdomains, where each subdomain Γ (Fig. 1d) is composed of six partial volumes (S_1^{+x}, S_1^{-x}, S_1^{+y}, S_1^{-y}, S_1^{+z}, and S_1^{-z}), corresponding to the spatial heterogeneity in the X, Y, and Z directions, as shown in Figs. 1c-1e
3: Computation of the mean directional entropies for each subdomain Γ_n, as $S_1^\zeta = (S_1^{+\zeta} + S_1^{-\zeta})/2$, for $\zeta = 1, 2$, and 3
4: Determination of the infimum and supremum of the set of all computed directional entropies for all N subdomains Γ.
5: Evaluation of the directional entropies at non-grid positions in the domain Ω by using the bicubic interpolation method. This operation is followed by mapping the resulting vector field containing the directional entropies to experimentally reported diffusivity coefficients (D_{WM}), determining the diffusion tensor $D_{ij}(x)$ for all voxels: $D(x) = [D_{11}\ 0\ 0,\ 0\ D_{22}\ 0,\ 0\ 0\ D_{33}]$
6: Imposition of a zero-flux boundary conditions for the elements located at the boundary surface $\partial\Omega$ (Eq. 6), and definition of the maximum cancer cell holding capacity at the center of the volume of interest Ω.
7: Discretization of the anisotropic parabolic equation and its corresponding boundary conditions (Eqs. 5 and 6) by using the FTCS. The truncation error of this scheme approaches to zero in the limit that $\delta t \to 0$, $\delta X \to 0$, assuming $\frac{\delta t}{(\delta x)^2} \leq \frac{1}{2}$ [15].

3. **Results.** The directional Shannon entropies, as well as the magnitude of the gradient of the resulting Shannon entropy were computed in different regions of the subcortical white matter. Obtained directional Shannon entropies are shown in Figs. 2a-2c for a specific region of the brain in the directions X, Y, and Z, respectively. In Fig. 2d, the magnitude of the gradient of the resulting Shannon entropy is plotted. At this specific brain location, a grid containing 27 subdomains with a radius $r = 0.25\ mm$ was used to characterize the cerebral tissue microstructure changes surrounding the GBM seed. As these plots demonstrate, entropies calculated in one direction segment can vary considerably depending on the reference location (e.g. approximately by a factor of two, as shown in Fig. 2b), suggesting a pronounced influence. Moreover, we note that in this special case the directional entropies S_1^x and S_1^y (Figs. 2a and 2b, respectively) are similar, however S_1^z yields

qualitatively different results, as can be noted visually from Fig. 2c. These changes in entropy within the $x-y$ plane versus the ones calculated in the orthogonal z direction are directly attributed to the diffusion anisotropy in our model. Therefore, symmetry is broken and the z direction turns out to be a distinguished direction for cell diffusion at this specific location. As a result, a scalar diffusion coefficient would be inadequate to capture these effects and anisotropy must be taken into account.

In Fig. 3, the progression of the three-dimensional spatial evolution of a glioblastoma multiforme after three months is shown using the estimated diffusivity tensor. It is important to note that the contours indicate the normalized concentration of tumor cells. We observe small but clearly discernible deviations from a spherical growth law as the distorted shape in Fig. 3b shows. These results indicate that diffusion anisotropy should be taken into account for realistic tumor morphology calculations.

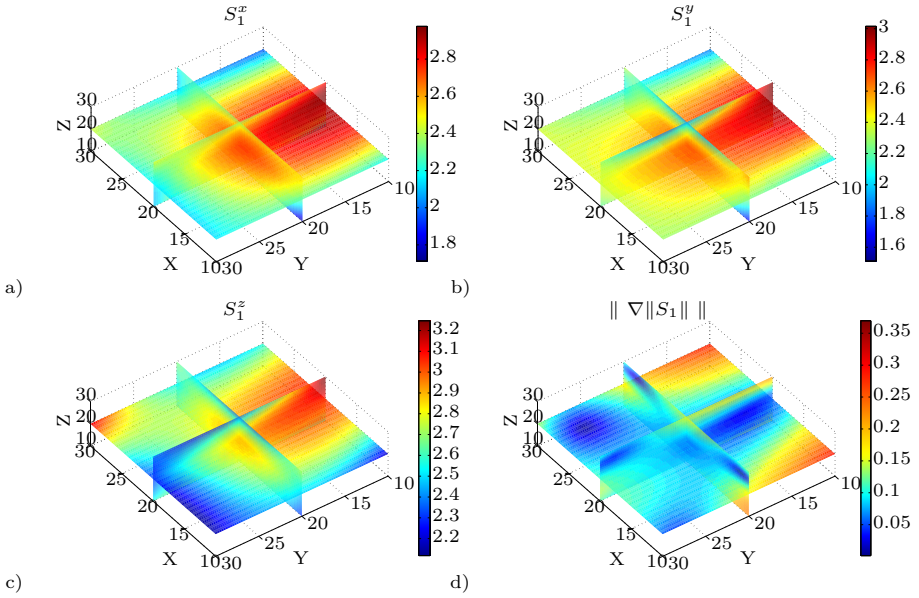

FIGURE 2. a) Resampled S_1^x Shannon entropy. b) Resampled S_1^y Shannon entropy. c) Resampled S_1^z Shannon entropy. d) Magnitude of the gradient of the resulting Shannon entropy: $\| \nabla \|S_1\| \| = \left[\left(\frac{\partial \|S_1\|}{\partial x} \right)^2 + \left(\frac{\partial \|S_1\|}{\partial y} \right)^2 + \left(\frac{\partial \|S_1\|}{\partial z} \right)^2 \right]^{\frac{1}{2}}$, where: $\|S_1\| = \left[(S_1^x)^2 + (S_1^y)^2 + (S_1^z)^2 \right]^{\frac{1}{2}}$. The directional entropies were resampled at regular intervals of $0.25 \times 0.25 \times 0.25\ mm^3$ using the bicubic interpolation method.

4. **Discussion.** Clinically, the identification of the origin of the tumor, staging, as well as its extension are very important parameters to be considered when modelling growth dynamics, which may be indirectly accessed by quantifying the glucose consumption (cells metabolic activity) revealed by positron emission tomography

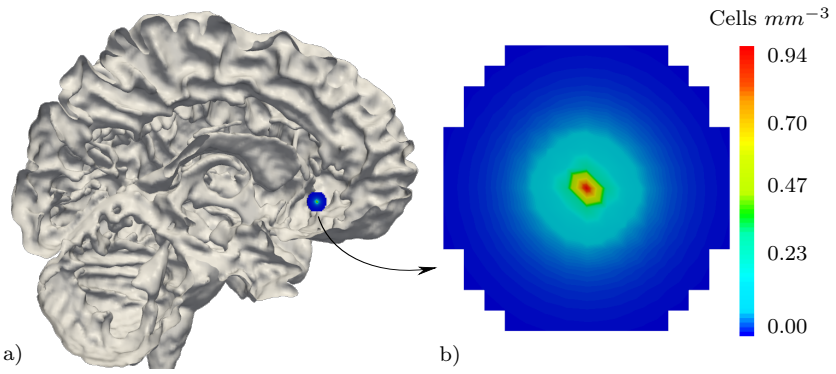

FIGURE 3. a) Three-dimensional simulation showing the progression of glioblastoma multiforme at three months. b) Contours indicate the normalized distribution of the tumor cells predicted by the mathematical model using the concept of directional entropies for quantification of different cerebral tissue microstructures and subsequent estimation of the diffusivity tensor.

(PET). For these reasons, the characterization of the different microstructures surrounding the tumor seed is highly desired. In this work, the estimation of the diffusivity tensor was achieved by calculating the directional entropies. By combining both the cancer cell diffusion gradients in different cerebral tissues and the brain tissue morphological complexity information, we can generate a map that allows us to convert the directional entropies obtained from MRI datasets into a numerical measure of diffusion, which reflects the macroscopic characteristics of tumor cell spread resulting from the microstructure surrounding the tumor seed in a patient-specific manner. The computed directional entropies were linearly mapped into experimental observed diffusivity coefficients, this theoretically assumed relationship is justified by the continuous transition of individual voxels from white to gray matter.

Our approach could also be used to model the possible development of a necrotic core, where the diffusion of nutrients at the center of the tumor is decreased below a critical level, which results in a decreased proliferation of tumor cells. This clinical condition most likely to generate a loss of structural organization induced by the abnormal growth of brain tissue and surrounding edematous brain, which is characterized by a higher entropy, thus consequently, by a relatively lower diffusivity. Finally, we believe that our methodology could be useful in understanding relationships between the spatial brain anisotropy with respect to the GBM's origin and their invasive potential. These relationships could be used to quantify the tumor aggressiveness in a given patient at a specific location, and could also be used as a tool for treatment planning optimization.

Acknowledgments. Special acknowledgement is due to Dr. Christian P. May for his detailed proofreading of the manuscript. The authors would like also to thank the anonymous reviewers for their helpful feedbacks and suggestions.

REFERENCES

[1] B. Brutovsky, D. Horvath and V. Lisy, Inverse geometric approach for the simulation of close-to-circular growth. The case of multicellular tumor spheroids, *Physica A: Statistical Mechanics and its Applications*, **387** (2008), 839–850.

[2] F. Camastra, Data dimensionality estimation methods: A survey, *Pattern Recognition*, **36** (2003), 2945–2954.

[3] P. Castorina and D. Zappalà, Tumor Gompertzian growth by cellular energetic balance, *Physica A: Statistical Mechanics and its Applications*, **365** (2006), 473–480.

[4] O. Clatz, M. Sermesant, P. yves Bondiau, H. Delingette, S. K. Warfield, G. Mal and N. Ayache, Realistic simulation of the 3d growth of brain tumors in mr images coupling diffusion with mass effect, *IEEE Transactions on Medical Imaging*, 1334–1346.

[5] C. A. Condat and S. A. Menchón, Ontogenetic growth of multicellular tumor spheroids, *Physica A: Statistical Mechanics and its Applications*, **371** (2006), 76–79.

[6] F. J. Esteban, J. Sepulcre, N. V. De Mendizábal, J. Goñi, J. Navas, J. R. De Miras, B. Bejarano, J. C. Masdeu and P. Villoslada, Fractal dimension and white matter changes in multiple sclerosis, *NeuroImage*, **36** (2007), 543–549.

[7] F. J. Esteban, J. Sepulcre, J. R. De Miras, J. Navas, N. V. De Mendizábal, J. Goñi, J. M. A. Quesada, B. Bejarano and P. Villoslada, Fractal dimension analysis of grey matter in multiple sclerosis, *Journal of the Neurological Sciences*, **282** (2009), 67–71.

[8] E. Fernández and H. F. Jelinek, Use of fractal theory in neuroscience: Methods, advantages, and potential problems., *Methods San Diego Calif*, **24** (2001), 309–321.

[9] A. Giese and M. Westphal, Glioma invasion in the central nervous system, *Neurosurgery*, **39** (1996), 235–250; discussion 250–252.

[10] C. Hogea, C. Davatzikos and G. Biros, Modeling glioma growth and mass effect in 3D MR images of the brain, *Medical Image Computing and Computer-Assisted Intervention*, **4791** (2007), 642–650.

[11] C. Hogea, C. Davatzikos and G. Biros, An image-driven parameter estimation problem for a reaction-diffusion glioma growth model with mass effects, *Journal of Mathematical Biology*, **56** (2008), 793–825.

[12] E. Izquierdo-Kulich, I. Rebelo, E. Tejera and J. M. Nieto-Villar, Phase transition in tumor growth: I avascular development, *Physica A: Statistical Mechanics and its Applications*, **392** (2013), 6616–6623.

[13] A. R. Kansal, S. Torquato, I. V. Harsh GR, E. A. Chiocca and T. S. Deisboeck, Simulated brain tumor growth dynamics using a three-dimensional cellular automaton., *Journal of theoretical biology*, **203** (2000), 367–382.

[14] R. D. King, B. Brown, M. Hwang, T. Jeon and A. T. George, Fractal dimension analysis of the cortical ribbon in mild Alzheimer's disease, *NeuroImage*, **53** (2010), 471–479.

[15] P. D. Lax, A stability theorem for solutions of abstract differential equations, and its application to the study of the local behavior of solutions of elliptic equations, *Communications on Pure and Applied Mathematics*, **9** (1956), 747–766.

[16] B. B. Mandelbrot, *The Fractal Geometry of Nature*, vol. 51, W. H. Freeman, 1982.

[17] J. D. Murray, *Mathematical Biology II: Spatial Models and Biomedical Applications (Interdisciplinary Applied Mathematics) (v. 2)*, Third edition. Interdisciplinary Applied Mathematics, 18. Springer-Verlag, New York, 2003.

[18] T. Neuvonen and E. Salli, Characterizing diffusion tensor imaging data with directional entropy., *Conference proceedings : ... Annual International Conference of the IEEE Engineering in Medicine and Biology Society. IEEE Engineering in Medicine and Biology Society. Annual Conference*, **6** (2005), 5798–5801.

[19] H. Ohgaki and P. Kleihues, Population-based studies on incidence, survival rates, and genetic alterations in astrocytic and oligodendroglial gliomas., *Journal of neuropathology and experimental neurology*, **64** (2005), 479–489.

[20] E. A. Reis, L. B. L. Santos and S. T. R. Pinho, A cellular automata model for avascular solid tumor growth under the effect of therapy, *Physica A: Statistical Mechanics and its Applications*, **388** (2009), 1303–1314.

[21] C. E. Shannon and W. Weaver, *The Mathematical Theory of Information*, vol. 97, University of Illinois Press, 1949.

[22] S. Sinha, M. E. Bastin, I. R. Whittle and J. M. Wardlaw, Diffusion tensor MR imaging of high-grade cerebral gliomas, *AJNR. American journal of neuroradiology*, **23** (2002), 520–7.

[23] G. S. Stamatakos, N. K. Uzunoglu, K. Delibasis, N. Mouravliansky, A. Marsh and M. Makropoulou, Tumor growth simulation and visualization: A review and a Web based paradigm., *Studies In Health Technology And Informatics*, **79** (2000), 255–274.

[24] T. Takahashi, T. Murata, M. Omori, H. Kosaka, K. Takahashi, Y. Yonekura and Y. Wada, Quantitative evaluation of age-related white matter microstructural changes on MRI by multifractal analysis., *Journal of the Neurological Sciences*, **225** (2004), 33–37.

[25] D. E. Woodward, J. Cook, P. Tracqui, G. C. Cruywagen, J. D. Murray and E. C. Alvord, A mathematical model of glioma growth: The effect of extent of surgical resection, *Cell Proliferation,* **29** (1996), 269–288.

Received June 10, 2015; Accepted October 29, 2015.

E-mail address: marcelo.eliasdeoliveira@epfl.ch; marcelo.ijk@gmail.com
E-mail address: goncalui@yahoo.com.br